Cardiac Glycosides. 4. A Structural and Biological Analysis of β-D-Digitoxosides, β-D-Digitoxose Acetonides, and Their Genins

Douglas C. Rohrer,*† Masaru Kihara,‡ Tamboue Deffo,‡ Hargovind Rathore,‡ Khalil Ahmed,§ Arthur H. L. From,§ and Dwight S. Fullerton‡

Contribution from the Medical Foundation of Buffalo, Inc., Buffalo, New York 14203, School of Pharmacy, Oregon State University, Corvallis, Oregon 97331, and Veterans Administration Medical Center, University of Minnesota, Minneapolis, Minnesota 55417.
Received February 17, 1984

Abstract: The structural and conformational characteristics of a series of five cardenolide analogues, their digitoxose acetonide derivatives, and their digitoxoside derivatives are determined from analysis of crystal structure results (including seven new structures reported here) and molecular mechanics calculations. The A, B, and C rings in the steroid backbone remain essentially conformationally invariant in all the structures, while the D rings show a high degree of flexibility. The conformational characteristics of the C17β side groups on the various analogues do not seem to be significantly affected by the nature of the C3 substituent. The bonds linking the steroid to the sugar moieties show a surprisingly small range of rotational freedom. The C2′–Cl′–O3–C3 torsion angles range only over 29.4° in 10 crystal structures, while the Cl′-O3–C3–C2 torsion angles range over 110.1°. A comparison of the structural characteristics of the "active" conformations of theses analogues and their derivatives with their potency as hog kidney Na^+,K^+-ATPase inhibitors reveals that the same type of linear relationship observed earlier for the genins exists for the glycoside derivatives. However, the addition of the sugar substituent enhances the potency in a specific way. The potencies of the digitoxose acetonide derivatives with the C3′ and C4′ oxygens blocked are increased systematically by a factor of 2, while the digitoxoside derivatives with free hydroxyls at C3′ and C4′ show a systematic potency enhancement of a factor of 10. These results are consistent with either O3′ or O4′ being involved in the enhancing process, but other earlier work indicates that the orientation of O4′ has the predominant influence.

Cardiac glycosides, particularly digoxin, continue to be widely used in medicine.[1,2] They are also important tools in the study of sodium/potassium dependent ATPase (Na^+,K^+-ATPase, E.C. 3.6.1.3), the enzyme which mediates the cellular sodium pump and thus performs a crucial role in a variety of vital physiological processes. Na^+,K^+-ATPase is specifically inhibited by cardiac glycosides and has been considered as the putative receptor for such drugs.[3] Our investigations have been directed toward determining how the structures and conformations of genins and cardiac glycosides contribute to their ability to inhibit Na^+,K^+-ATPase[4-6] and alter inotropic activity.[7]

We have previously reported that the relative position of the C17β-side-group carbonyl oxygen (or nitrile nitrogen) on a variety of digitalis genin analogues can be used to accurately predict Na^+,K^+-ATPase inhibitory activity of these molecules[4-6] and their inotropic activity.[7] These analyses have now been extended to include the influence of the cardiac glycoside's sugar structure and conformation on the biological activity. Initial results indicate an unexpected and major role for the sugar's 4′-OH position (equatorial vs. axial) in determining the relative activity of monoglycoside derivatives. It is noteworthy that the model of Yoda and Yoda[8,9] had emphasized the importance of the sugar's 3′-OH position.

This paper reports a comparison of the structural features of five genin analogues (Ia–Va), their corresponding β-D-digitoxose acetonides (Ib–Vb), and their β-D-digitoxosides (Ic–Vc) with their hog kidney Na^+,K^+-ATPase inhibitory potency. Syntheses of these glycosides have been reported recently.[1] The X-ray crystal structures of seven digitalis analogues are reported: genins IIa and IIIa, β-D-digitoxose acetonides Ib, IIb, IIIb, and (20*S*)-IVb, and β-D-digitoxoside IIc. These structures together with other published crystal structures provide the foundation for the analyses described.

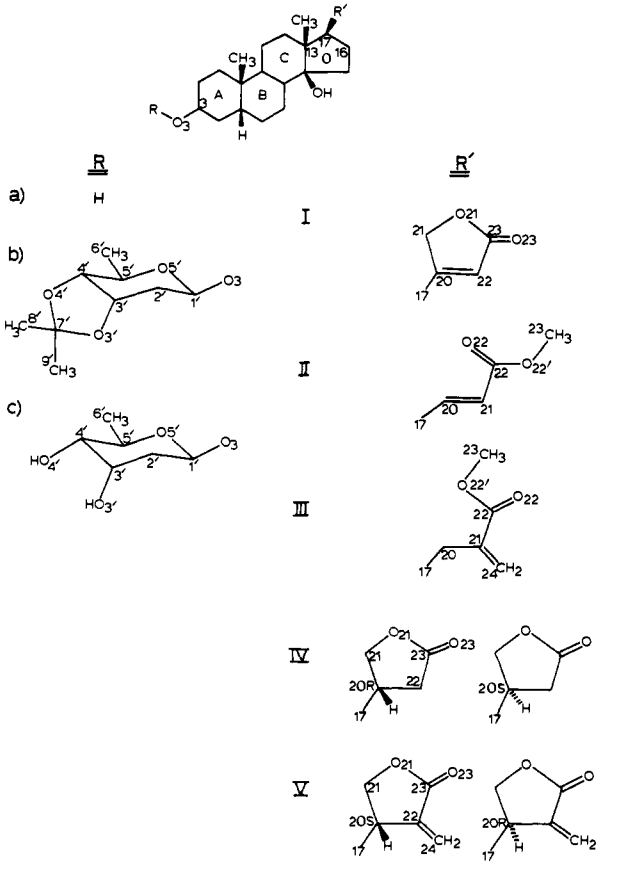

Results and Discussion

The results obtained from studies on a series of cardioactive genins[1,4-7] have clearly shown that the structures and conformations of these molecules play an important role in determining their Na^+,K^+-ATPase inhibitory potency. A correlation between

* Present address: The Upjohn Co., Kalamazoo, MI 49001.
† Medical Foundation of Buffalo, Inc.
‡ Oregon State University.
§ Veterans Administration Medical Center.

(1) Paper 3 in this series: Kihara, M.; Yoshioka, K.; Deffo, T.; Fullerton, D. S.; Rohrer, D. C. *Tetrahedron* **1984**, *40*, 1121–1133.
(2) Gilman, G., Goodman, L., Gilman, A., Eds., "The Pharmacological Basis of Therapeutics", 6th Ed.: MacMillan: New York, 1980.

0002-7863/84/1506-8269$01.50/0

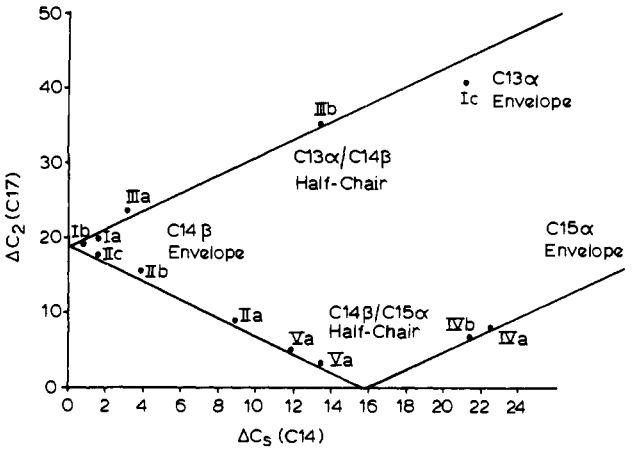

Figure 1. D-ring principal asymmetry parameters; ΔC_2(C17), the two-fold rotation parameter through C17, is plotted vs. ΔC_s(C14), the mirror parameter through C14.

the relative location of the carbonyl oxygen on the C17β substituent and activity was observed. Those results provided the basis for choosing the five genins, Ia–Va, used in these and the previously reported[1,4-7] studies on the corresponding glycosides. The inhibitory activities of these genins toward hog kidney Na^+,K^+–ATPase range in value from 1.08×10^{-7} M for IIa to 1.2×10^{-5} M for (20*S*)-Va.

Molecular Structure Analysis. Crystal Structures. Molecular structure data obtained from crystal structure determinations have been used as the basis for all comparisons and molecular mechanics calculations described here. The structures of genins IIa and IIIa together with the previously published crystal structures of Ia,[10] (20*S*)-IVa,[4] and (20*S*)-Va[4] provide a complete series of genin structures for the glycoside derivatives chosen for these studies. The crystal structures of the β-D-digitoxose acetonides Ib, IIb, IIIb, and (20*S*)-IVb are also reported here, providing another nearly complete series. In addition, the crystal structure of the β-D-digitoxoside IIc is reported, which in combination with the published structure of the β-D-digitoxoside of digoxigenin[11] (I'c) provides two monodigitoxoside structures for precise comparison. These structural results represent the three classes of analogue under examination: the genin analogue without a sugar, the digitoxose acetonide deriatives with O3' and O4' blocked, and the digitoxoside derivatives with free hydroxyl groups at C3' and C4'.

Steroid Backbone Structure. Comparison of the structural parameters for the steroid backbones in the seven structures reported here with previously published structures shows very good agreement. In every case, the A, B, and C rings have a standard chair conformation. The D rings, however, exhibit a great deal of conformational flexibility. The conformational asymmetry parameters[12] allow these conformational variations to be evaluated and graphically represented (Figure 1). These results are consistent with earlier observations about conformational flexibility of genin D rings.[13] However, the conformational trends relating

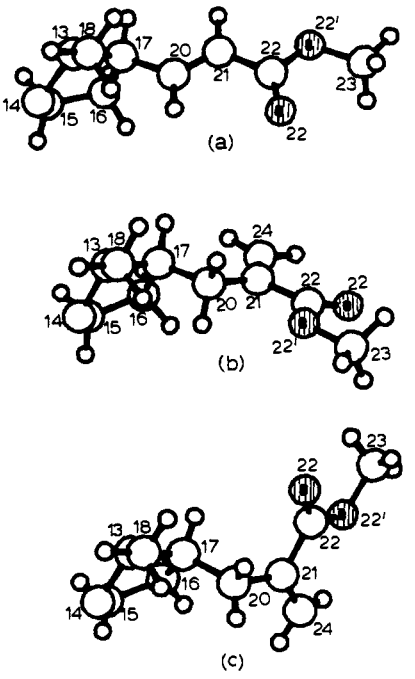

Figure 2. Perspective drawings of the C17β side group and D ring in the structure of (a) the acyclic α,β-unsaturated methyl ester, (b) the α-methylene methyl ester in the "active" conformation, and (c) the α-methylene methyl ester in an alternate conformation.

the nature of the C17β side group to preferred D-ring conformation must be modified to incorporate the additional data now available. The modified lactone substituents of analogue IV and V are correlated with the D ring in a C14β/C15α-half-chair conformation, but the range of variation is somewhat larger than earlier data indicated. The D rings of molecules substituted with the planar lactone, I, appear to prefer a C14β-envelope conformation but are not restricted to this conformation (see Ic in Figure 1). The analogues with acyclic substituents, II and III, show no preference in D-ring conformation.

C17β-Side-Group Orientations. It has been shown that the relative location of the carbonyl oxygen on the genin C17β side group plays a vital role in determining the relative biological activities of these analogues both as inhibitors of Na^+,K^+-ATPase[1,4-6] and as inotropic agents.[7] A quantitative measure of the relative position of an analogue's carbonyl oxygen was obtained by superimposing the atoms in the steroid backbone upon the corresponding atoms in the prototype digitoxigenin, Ia, then calculating the oxygen–oxygen separation.[14] In the cases where the analogues were found to be more active than the prototype, a negative oxygen–oxygen distance was determined to provide continuity of the linear relationship observed between structure and activity. Therefore, an analysis of the side-group orientation and conformations of these glycoside derivatives is important to understand their activity. The most obvious questions to be answered are, first, whether the carbonyl oxygen position is as much a determinant of glycoside activity as it is of genin activity and, second, what effect does the presence of the sugar moiety have on the preferred conformation of the C17β side group and, in particular, the relative position of the carbonyl oxygen?

The planar lactone side group of the prototype genin digitoxigenin (Ia) has two low-energy orientations relative to the steroid backbone which are related by a 180° rotation about the C17–C20 bond.[14] The structural nature of receptor theory would predict that only one of these two orientations should provide optimal binding to the receptor and high activity. Studies using analogues with less rotational freedom have shown that this is the case with the genins and that the "active" orientation for digitoxigenin has

(3) Hoffman, J. F., Forbush B., III, Eds., "Structure and Function of the Na/K Pump;" Academic Press: New York, 1983; Vol 19.
(4) Rohrer, D. C.; Fullerton, D. S.; Yoshioka, K.; Kitatsuji, E.; Ahmed, K.; From, A. H. L. *Acta Crystallogr., Sect. B* **1983**, *B39*, 272–280.
(5) Ahmed, K.; Rohrer, D. C.; Fullerton, D. S.; Deffo, T.; Kitatsuji, E.; From, A. H. L. *J. Biol. Chem.* **1982**, *258*, 8092–8097.
(6) Fullerton, D. S.; Kihara, M.; Deffo, T.; Kitatsuji, E.; Ahmed, K.; Simat, B.; From, A. H. L.; Rohrer, D. C. *J. Med. Chem.* **1984**, *27*, 256–261.
(7) From, A. H. L.; Fullerton, D. S.; Deffo, T.; Kitatsuji, E.; Rohrer, D. C.; Ahmed, K. *J. Mol. Cell. Cardiol.*, in press.
(8) Yoda, A. *Ann. N.Y. Acad. Sci.* **1974**, 598–616.
(9) Yoda, A.; Yoda, S. *Mol. Pharmacol.* **1975**, *11*, 653–662.
(10) Karle, I. L.; Karle, J. *Acta Crystallogr., Sect. B* **1969**, *B25*, 4434–4442.
(11) Go, K.; Kartha, G. *Cryst. Struct. Commun.* **1982**, *11*, 279–284.
(12) Duax, W. L.; Weeks, C. M.; Rohrer, D. C. *Top. Stereochem.* **1976**, *9*, 271–383.
(13) Rohrer, D. C.; Fullerton, D. S.; Yoshioka, K.; From, A. H. L.; Ahmed, K. In "Computer Assisted Drug Design"; Olson, E. C., Christoffersen, R. E., Eds.; American Chemical Society: Washington, DC, 1979; pp 259–279.
(14) Rohrer, D. C.; Fullerton, D. S. *Acta Crystallogr., Sect. B* **1980**, *36*, 1565–1568.

a C13—C17—C20═C22 torsion angle, χ, of approximately 76°. The crystal-structure results for the digitoxose acetonide Ib and the digoxigenin digitoxoside have the alternate orientation for the lactones with χ values of −114.3 and −95.7°, respectively, which would place the carbonyl oxygen more than 2 Å from the "active" position of the prototype Ia. However, rotation of the lactone to the alternate minimum-energy conformation with χ = 76° brings the carbonyl oxygen of Ib to a position only 0.39 Å away from carbonyl oxygen position of the prototype Ia. Applying the same type of rotation to the digoxigenin digitoxoside analogue reduces the separation from Ia's position to 0.89 Å, very close to the 0.69-Å distances observed for digoxigenin itself.[13] Thus, the presence of a sugar does not seem to significantly alter the relative position of the carbonyl oxygen position of the digitoxigenin analogues' C17β side group.

The crysal structures of methyl ester IIa, its digitoxose acetonide IIb, and its digitoxoside IIc also have very similar C17β-side-group orientations and conformations. The χ values, −135.5°, −126.9°, and −125.1°, are all well within the minimum energy range for this genin side group.[13] Furthermore, all the C17β side groups have their α,β-unsaturated systems in a cisoid arrangement (Figure 2a) with C20═C21—C22═O22 torsion angles of −7.1°, −12.2°, and −7.1°, and an extended methoxy conformation with C21—C22—O22′—C23 torsion angles of −175.4°, −177.9°, and −175.5°. This means that all of the C17β-side-group atoms are nearly coplanar. Comparing the relative locations of the carbonyl oxygens of these three analogues to the relative location of the oxygen in Ia shows very little variation in position, 1.42, 0.95 and 0.90 Å, again indicating that the addition of a sugar moiety has little effect on the carbonyl oxygen position critical for the biological activity of the glycoside molecule.

The C17β side groups of the α-methylene methyl ester IIIa and its digitoxose acetonide IIIb are much more flexible. The χ values for the genin and digitoxose acetonide are similar, −177.8° and −171.7°, and the methoxy portions of the esters are both extended; C21—C22—O22′—C23 are −178.3° and −178.4°. That, however, is where the similarity ends. The single bond between C20 and C21 affords freedom of rotation in the side chain not present in the other analogues. The C17—C20—C21—C22 torsion in the genin IIIa is −174.4° which is similar to the side chain of II with a C20—C21 trans-double-bond structure (Figure 2b). However, this angle in the structure of the digitoxose acetonide IIIb is 77.8° (Figure 2c). Further, while the genin C20—C21—C22═O22 torsion angle is 175.0°, that angle in the acetonide is 13.1°. This also indicates that while the α,β-unsaturated system of genin IIIa is cisoid with a C24═C21—C22═O22 torsion angle of −4.4°, the acetonide IIIb has a transoid conjugated system with a corresponding torsion angle of −165.3°.

These differences graphically demonstrate the conformational variability of this side group. While both observed conformations for the C17β side group of III represent minimum-energy structures, one of the orientations should provide a better fit at the Na^+,K^+-ATPase binding site than the other. Since the orientation of IIIa has the carbonyl oxygen closer, 2.48 Å, to the relative location of the oxygen in digitoxigenin than that of IIIb, 4.14 Å, the orientation observed in IIIa is taken to be the "active" conformation. If the conformation of the C17β side group on the digitoxose acetonide is twisted to mimic that of the genin, the relative location of the carbonyl oxygens becomes 2.46 Å.

Digitoxoside and Digitoxose Acetonide Conformations. The addition of the acetonide group significantly flattens the chair conformation of the unsubstituted digitoxoside hexopyranosyl ring. The C1′–C2′–C3′–C4′ and C2′–C3′–C4′–C5′ intra-ring torsion angles are reduced on the average by 12.6° and −13.4°, respectively. As expected, the exocyclic torsion angles involving O3′ and O4′ are also significantly altered by the addition of the acetonide. A more detailed discussion of the structural and conformational features of the digitoxoside and digitoxoside acetonide moieties has been published elsewhere.[15]

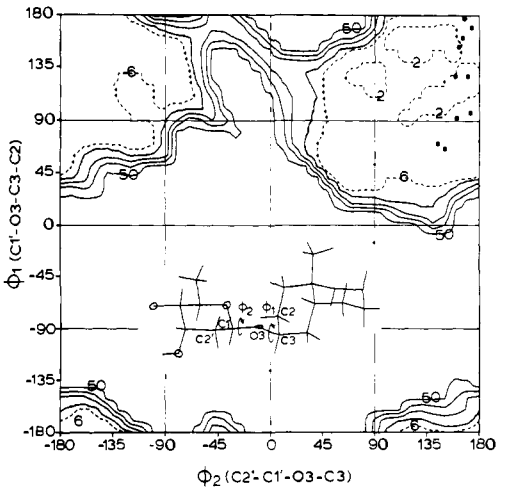

Figure 3. Potential energy contour map for the rotation of the sugar–steroid linkage bonds in Ic. The dashed contour lines represent the isoenergy levels of 2 and 6 kcal/mol, while the solid contour lines represent the isoenergy levels 10, 20, 30, and 50 kcal/mol. The locations of the 10 cardiac glycoside crystal structure conformations are represented on the contour map as solid circles.

Table I. β-D-Sugar–Steroid Linkage Torsion Angles

analogue	ϕ_1, deg	ϕ_2, deg	sugar
Ib	169.9	173.3	β-D-digitoxose acetonide
IIb	98.6	170.9	β-D-digitoxose acetonide
IIIb	129.4	159.1	β-D-digitoxose acetonide
(20*S*)-IVb	92.7	159.8	β-D-digitoxose acetonide
I′c	161.8	165.2	β-D-digitoxoside
IIc	154.1	161.4	β-D-digitoxoside
actodigin[17]	177.6	167.5	β-D-glucoside
digoxigenin bisdigitoxoside[18]	70.9	143.9	di-β-D-digitoxoside
digoxin[19]	67.5	149.8	tri-β-D-digitoxoside
gitoxin[20]	128.5	169.9	tri-β-D-digitoxoside

Sugar–Steroid Conformations. The first sugar attached to the genin has the greatest effect on binding and activity.[16] Thus, its orientation relative to the steroid is of primary importance when developing structural models that explain the specificity of a particular sugar for the "sugar binding site" of Na^+,K^+-ATPase. Potential energy calculations for rotation about the two bonds linking the steroid backbone and the sugar moieties in the digitoxoside Ic (Figure 3) show that more than two-thirds of the conformations obtained by rotating 360° about each bond are forbidden due to unfavorable nonbonded contacts.

The conformations (Table I), for the six glycoside crystal structures reported here all fall into the lower energy regions of the conformational energy maps. The orientations about the C3–O3 bond (i.e., C2–C3–O3–C1′, ϕ_1) show a rather wide range of values, 77.2°, which extend across the full range of the allowed ϕ_1 region (Figure 3). The range of orientation about the O3–C1′ (i.e., C3–O3–C1′–C2′, ϕ_2), however, is surprisingly small, only 14.2°. The range for rotation of the O3–C1′ bond covers only a small portion of the allowed ϕ_2 region. Comparison of these observations with the crystal-structure results on four additional cardiac glycosides, actodigin,[17] digoxigenin bisdigitoxoside,[18] digoxin,[19] and gitoxin,[20] shows that this conformational trend exists for all 10 structures. The values (Table I) for ϕ_1 extend from

(15) Kihara, M.; Yoshioka, K.; Kitatsuji, E.; Hashimoto, T.; Fullerton, D. S.; Rohrer, D. C. *Steroids* **1983**, *44*, 37–53.

(16) Yoda, A.; Yoda, S.; Sarrif, A. M. *Mol. Pharmacol.* **1973**, *9*, 766–773.
(17) Fullerton, D. S.; Yoshioka, K.; Rohrer, D. C.; From, A. H. L.; Ahmed, K. *Mol. Pharmacol.* **1979**, *17*, 43–51.
(18) Go, K.; Kartha, G. *Cryst. Struct. Commun.* **1982**, *11*, 285–290.
(19) Go, K.; Kartha, G.; Chen, J. P. *Acta Crystallogr., Sect. B* **1980**, *B36*, 1811–1819.
(20) Go, K.; Kartha, G. *Acta Crystallogr., Sect. B* **1980**, *36*, 3034–3040.
(21) Messerschmidt, A. *Cryst. Struct. Commun.* **1980**, *9*, 1185–1194.
(22) Go, K.; Kartha, G. *Cryst. Struct. Commun.* **1981**, *10*, 1329–1334.
(23) Kartha, G.; Go, K. *Cryst. Struct. Commun.* **1981**, *10*, 1323–1327.

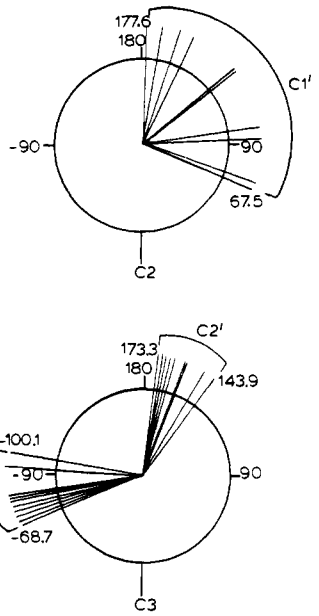

Figure 4. Newman projections down the C3–O3 and O3–C1′ sugar–steroid linkage bonds in the crystal structures of 10 cardiac glycosides.

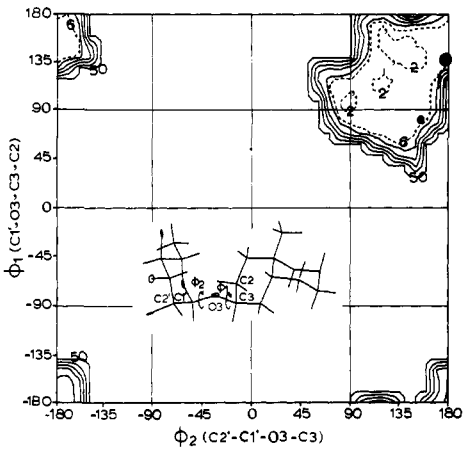

Figure 5. Potential energy contour map for the rotation of the sugar–steroid linkage bonds in digitoxigenin α-L-*rhamno*-hexopyranoside. The dashed contour lines represent the isoenergy levels of 2 and 6 kcal/mol, while the solid contour lines represent the isoenergy levels 10, 20, 30, and 50 kcal/mol. The locations of the three crystal structure conformations are represented as solid circles.

Table II. α-L-Rhamnose–Steroid Analogue Linkage Torsion Angles

analogue	ϕ_1, deg	ϕ_2, deg
ouabain octahydrate[21]	160.4	176.8
ouabain diethanol[22]	159.9	174.4
oleandrin[23]	79.9	153.5

67.5° to 177.6°, or a range of 110.1°, while ϕ_2 is limited to values from 143.9° to 173.3°, or a range of only 29.4°. The Newman projections for ϕ_1 and ϕ_2 (Figure 4) graphically illustrate the differences in conformational flexibility exhibited by two linking bonds.

An even more dramatic example of the limited conformational range of sugar–steroid bond rotation has been found for rotation of the α-L-rhamnose-like sugars (Figure 5). This is a result of the shift of an axial linkage in the α-L sugars compared to the equatorial linkage of the β-D sugars. The crystal-structure results for analogues containing α-L-sugar moieties, however, do show the same conformational trends observed for the β-D-sugar structures. The ϕ_1 and ϕ_2 values in the crystal structures of three α-L-rhamnose analogues, given in Table II, reveal a range of 80.5° for ϕ_1, while the ϕ_2 range is only 26.5°.

Table III. Relative C17β-Side-Group Carbonyl Oxygen Distances

	carbonyl oxygen distances, Å		
analogue	genins	digitoxose acetonides	digitoxoside
I	0.0Å	0.39Å	
I′	0.64		0.89Å
II	−1.42	−0.95	−0.9
III	2.48	2.47	
(20*S*)-IV	2.91	2.81	
(20*S*)-V	4.98		

Table IV. Hog Kidney Na^+,K^+-ATPase Inhibition Data

	hog kidney Na^+,K^+-ATPase I_{50}, M		
analogue	genins	digitoxose acetonides	digitoxoside
I	1.3×10^{-7}	4.18×10^{-8}	7.0×10^{-9}
I′	3.0×10^{-7}		
II	1.5×10^{-7}	9.9×10^{-8}	2.98×10^{-8}
III	3.4×10^{-6}		3.06×10^{-7}
(20*S*)-IV	5.3×10^{-6}	1.74×10^{-6}	2.32×10^{-7}
(20*R*)-IV	7.28×10^{-6}	2.98×10^{-6}	5.17×10^{-7}
(20*S*)-V	1.2×10^{-5}	6.91×10^{-6}	9.28×10^{-7}
(20*R*)-V	1.34×10^{-5}	3.45×10^{-5}	2.8×10^{-6}

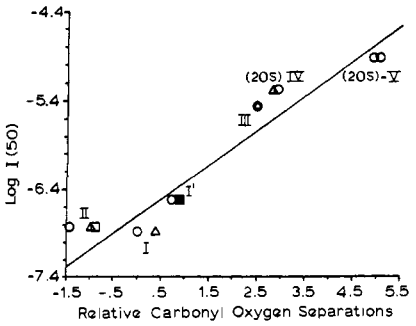

Figure 6. The relative distance between the C17β-side-group carbonyl oxygen position in the "active" conformation on the representative genins (○), digitoxose acetonide derivatives (□), digitoxoside derivatives (△), and the carbonyl oxygen on the prototype digitoxigenin Ia vs. log $[I_{50}]$ for the genins. The line, log $[I_{50}] = 0.3D - 6.6$, is the regression fit line to the genin data.

The small range of values observed for ϕ_2, however, can be explained if electronic effects are considered in addition to the nonbonded interaction energies calculated by molecular mechanics. Ab initio molecular orbital calculations have been performed on a series of model systems to examine the electronic nature of the anomeric effect in pyranoses.[24-27] These calcuations have shown that the orientation corresponding to a ϕ_2 value of approximately 180° for the β-glycosidic bond is favored by 1 kcal/mol over the next lowest minimum-energy conformation corresponding to a ϕ_2 value of about −60°.[26] The calculations were not detailed enough to explain the consistent negative shift in the orientation to an average ϕ_2 of 162 ± 9°. Calculations on the α-glycoside bond show a similar type of conformational preference corresponding to a ϕ_2 value of about 180°. In this case the minimum is 2.6 kcal/mol lower in energy than the next lowest minimum-energy conformation.[27] The crystallographically observed conformations are consistent with the calculations on the models.

Structure and Activity. Role of Carbonyl Oxygen Position in Glycoside Activity. As described above (C17β-Side-Group Orientations), addition of a digitoxose acetonide or digitoxoside to digitoxigenin, Ia, digoxigenin, Ia′, the α,β-unsaturated methyl ester

(24) Jeffrey, G. A.; Pople, J. A.; Radom, L. *Carbohydr. Res.* **1972**, *25*, 117–131.
(25) Jeffrey, G. A.; Pople, J. A.; Radom, L. *Carbohydr. Res.* **1974**, *38*, 81–95.
(26) Jeffrey, G. A.; Yates, J. H. *Carbohydr. Res.* **1981**, *96*, 205–213.
(27) Jeffrey, G. A.; Pople, J. A.; Binkley, J. S.; Vishveshwara, S. *J. Am. Chem. Soc.* **1978**, *100*, 373–379.

Table V. Atomic Coordinates ($\times 10^4$) and Equivalent Isotropic Thermal Parameters ($\times 10^2$) for Ib[a]

	x	y	z	B_{iso}
C(1)	11446 (3)	9545 (2)	2380 (7)	511 (13)
C(2)	11230 (3)	9163 (3)	960 (6)	563 (15)
C(3)	10376 (2)	8915 (2)	1269 (6)	421 (10)
C(4)	10338 (2)	8671 (2)	3067 (6)	355 (9)
C(5)	10580 (2)	9049 (1)	4532 (4)	292 (7)
C(6)	10527 (3)	8783 (3)	6322 (6)	513 (13)
C(7)	11231 (2)	8390 (2)	6605 (7)	486 (12)
C(8)	12097 (2)	8623 (1)	6320 (5)	303 (7)
C(9)	12145 (2)	8884 (1)	4497 (5)	293 (7)
C(10)	11444 (2)	9304 (1)	4250 (5)	313 (8)
C(11)	13023 (2)	9110 (2)	4176 (7)	521 (13)
C(12)	13688 (3)	8684 (3)	4429 (7)	538 (14)
C(13)	13688 (2)	8434 (2)	6255 (6)	375 (9)
C(14)	12802 (2)	8224 (1)	6669 (5)	357 (9)
C(15)	12746 (4)	7711 (2)	5607 (12)	664 (19)
C(16)	13614 (5)	7467 (3)	5776 (19)	1038 (34)
C(17)	14229 (3)	7920 (2)	6182 (8)	572 (14)
C(18)	14001 (3)	8835 (2)	7591 (8)	504 (13)
C(19)	11551 (4)	9778 (2)	5503 (10)	588 (16)
C(20)	14779 (3)	7801 (2)	7712 (8)	495 (12)
C(21)	14489 (4)	7632 (3)	9475 (11)	712 (20)
C(22)	15610 (3)	7790 (2)	7726 (10)	595 (16)
C(23)	15905 (4)	7625 (2)	9419 (11)	711 (19)
O(3)	9792 (2)	9351 (1)	1095 (4)	423 (7)
O(14)	12823 (2)	8097 (1)	8494 (5)	559 (10)
O(21)	15245 (3)	7533 (2)	10449 (7)	814 (14)
O(23)	16617 (3)	7556 (2)	9915 (9)	1027 (19)
C(1′)	8949 (2)	9218 (2)	1036 (5)	366 (9)
C(2′)	8461 (3)	9720 (2)	1074 (9)	491 (12)
C(3′)	7539 (3)	9637 (2)	706 (8)	527 (13)
C(4′)	7358 (3)	9223 (2)	−663 (7)	544 (13)
C(5′)	7962 (3)	8760 (2)	−648 (7)	492 (12)
C(6′)	7904 (5)	8422 (4)	−2298 (12)	821 (24)
C(7′)	6369 (3)	9191 (3)	1602 (10)	744 (20)
C(8′)	6192 (7)	8711 (5)	2716 (19)	1073 (37)
C(9′)	5668 (5)	9597 (7)	1530 (22)	1201 (51)
O(3′)	7124 (2)	9430 (2)	2205 (5)	587 (10)
O(4′)	6544 (2)	9045 (2)	−189 (7)	805 (14)
O(5′)	8804 (2)	8952 (1)	−569 (4)	461 (7)

[a] $B_{iso} = {}^4/_3\sum_i\sum_j\beta_{ij}(a_ia_j)$. The esd's are given in parentheses.

IIa, or the α-methylene methyl ester IIIa does not appear to significantly alter the position of the low-energy conformations for the C17β side groups. Therefore, essentially the same carbonyl oxygen position observed for the genin structures can be obtained in the glycoside structures. Although more crystal-structure data will be needed to confirm this observation, the data for the six glycosides in Table III show a strong similarity between the C17β-side-group conformations of the glycosides and the corresponding genins. These distance data also give some estimate of the range of conformational variation that is possible for the relative position of the carbonyl oxygen. Figure 6 shows the distance data for the genins, digitoxosides, and the digitoxose acetonides plotted against the genin I_{50} data for hog kidney Na^+,K^+-ATPase (Table IV). The regression analysis line fit to the genin data was also plotted. The r^2 for the seven non-genin points was 0.93 and the s value was 0.26. The largest group of distances involved genin IIa with a variation of only 0.52 Å. Thus, addition of the sugar moiety does not significantly influence the conformation of the steroid or the orientation of the C17β side groups since there is a minimum-energy conformation for the glycosides where the carbonyl oxygen positions correspond well with those observed for the genin structure.

Role of the Sugar in Glycoside Activity. Since the genin position of the glycosides appears to make the same contribution to activity with or without a sugar, the next step was to factor out the sugars' contribution to glycoside activity. Table IV contains the hog kidney Na^+,K^+-ATPase I_{50} data for the three genins, digitoxosides, and digitoxose acetonides. Plotting these I_{50} data against the relative carbonyl oxygen position data (Figure 7) the same linear relationship found with the genins was observed for each series of derivatives but with an enhancement of activity associated with

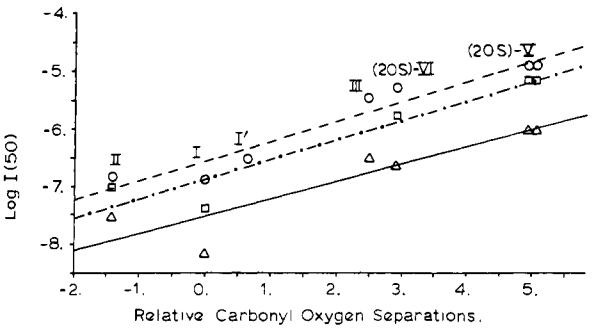

Figure 7. The relative distance between the C17β-side-group carbonyl oxygen position of the representative genin analogues (○), digitoxose acetonide derivatives (□), digitoxoside derivatives (△), and the carbonyl oxygen on the prototype digitoxigenin Ia *vs.* log [I_{50}] for the corresponding class of derivatives. The lines are the corresponding regression fit lines.

Table VI. Atomic Coordinates ($\times 10^5$) and Equivalent Isotropic Thermal Parameters ($\times 10^2$) for IIa[a]

	x	y	z	B_{iso}
C(1)	46711 (12)	89862 (11)	17135 (32)	340 (5)
C(2)	48465 (13)	92467 (11)	36644 (37)	370 (5)
C(3)	50893 (12)	86231 (11)	49157 (30)	340 (5)
C(4)	44815 (12)	79929 (11)	48125 (29)	309 (4)
C(5)	43289 (13)	77154 (10)	28544 (30)	304 (4)
C(6)	37247 (13)	70716 (10)	28486 (36)	368 (5)
C(7)	28755 (13)	73205 (11)	33811 (34)	355 (5)
C(8)	25737 (12)	79663 (11)	22070 (29)	297 (4)
C(9)	31904 (12)	86135 (10)	21442 (28)	274 (4)
C(10)	40442 (12)	83513 (11)	15648 (28)	295 (4)
C(11)	28484 (12)	92354 (11)	9472 (32)	325 (5)
C(12)	20389 (12)	95089 (10)	16780 (31)	311 (4)
C(13)	13807 (12)	89065 (11)	17768 (27)	286 (4)
C(14)	17300 (12)	82238 (10)	28335 (27)	278 (4)
C(15)	16575 (12)	84569 (10)	48411 (28)	317 (5)
C(16)	8483 (14)	88582 (13)	49622 (29)	368 (5)
C(17)	6924 (12)	92046 (10)	30353 (30)	316 (4)
C(18)	11057 (14)	87248 (12)	−1746 (30)	363 (5)
C(19)	40599 (15)	80902 (15)	−4492 (33)	412 (5)
C(20)	−1618 (13)	90625 (11)	24830 (31)	350 (5)
C(21)	−7357 (14)	95616 (12)	25396 (36)	403 (5)
C(22)	−15910 (13)	93974 (13)	22020 (37)	425 (6)
C(23)	−29215 (16)	98944 (18)	23989 (55)	650 (9)
O(3)	58815 (8)	83759 (8)	43895 (24)	401 (3)
O(14)	11746 (9)	76062 (7)	26171 (20)	318 (3)
O(22)	−18639 (11)	88089 (10)	16744 (33)	603 (5)
O(22′)	−20501 (10)	99851 (10)	25343 (32)	567 (5)
O(W)	−34084 (10)	80869 (11)	8810 (30)	594 (5)

[a] $B_{iso} = {}^4/_3\sum_i\sum_j\beta_{ij}(a_ia_j)$. The esd's are given in parentheses.

addition of the sugar. Linear regression analysis of the digitoxose acetonide and digitoxoside data results showed a relatively uniform contribution of each sugar:

Genins

$$\log [I_{50}] = [0.34\ (\pm 0.04)]D - 6.6\ (\pm 0.1) \qquad r^2 = 0.93,\ s = 0.26,\ n = 7$$

β-D-Digitoxose acetonides:

$$\log [I_{50}] = [0.34\ (\pm 0.06)]D - 6.9\ (\pm 0.2) \qquad r^2 = 0.91,\ s = 0.36,\ n = 5$$

β-D-Digitoxosides

$$\log [I_{50}] = [0.30\ (\pm 0.07)]D - 7.5\ (\pm 0.2) \qquad r^2 = 0.82,\ s = 0.40,\ n = 6$$

The regression fit lines for the three types of derivatives are clearly parallel with slopes of 0.34, 0.30, and 0.34, providing additional support for independence of the sugar effects from that of the C17β side groups; that is, the sugars increase genin activity by a constant factor. Figure 7 shows that addition of a β-D-digitoxose acetonide increases genin hog kidney Na^+,K^+-ATPase I_{50} activity by an average of 2.1 times while addition of a β-D-digitoxose increases

Table VII. Atomic Coordinates ($\times 10^5$) and Equivalent Isotropic Thermal Parameters ($\times 10^2$) for IIb[a]

	x	y	z	B_{iso}
C(1)	28553 (17)	90391 (10)	38788 (24)	488 (5)
C(2)	26342 (22)	85243 (9)	32817 (26)	519 (6)
C(3)	20499 (20)	85664 (8)	19612 (24)	492 (5)
C(4)	9787 (20)	88841 (10)	20626 (25)	509 (6)
C(5)	11761 (18)	94002 (9)	27049 (21)	464 (5)
C(6)	536 (25)	96946 (11)	28121 (26)	580 (7)
C(7)	−7451 (19)	94640 (12)	38299 (24)	535 (6)
C(8)	−1803 (16)	94192 (8)	51992 (20)	402 (4)
C(9)	9648 (15)	91346 (7)	51102 (19)	376 (4)
C(10)	17785 (16)	93640 (7)	40585 (21)	413 (4)
C(11)	15049 (17)	90933 (10)	64787 (22)	480 (5)
C(12)	7002 (20)	88399 (11)	74630 (25)	521 (6)
C(13)	−4485 (17)	91142 (8)	76052 (21)	449 (5)
C(14)	−9898 (16)	91874 (8)	62230 (21)	431 (4)
C(15)	−14398 (22)	86606 (10)	59040 (28)	544 (6)
C(16)	−19254 (32)	84681 (13)	71992 (36)	731 (9)
C(17)	−12725 (21)	87421 (9)	83283 (27)	529 (6)
C(18)	−2860 (25)	96074 (10)	83578 (25)	535 (6)
C(19)	21914 (27)	98919 (10)	44956 (31)	588 (7)
C(20)	−20967 (19)	89779 (9)	92643 (24)	494 (5)
C(21)	−22185 (19)	88384 (9)	105055 (25)	491 (5)
C(22)	−30934 (17)	90571 (8)	113636 (23)	460 (5)
C(23)	−40624 (33)	89604 (19)	133803 (39)	794 (11)
O(3)	27945 (13)	88082 (5)	10036 (16)	478 (3)
O(14)	−19957 (13)	94914 (7)	63432 (19)	551 (4)
O(22)	−36533 (17)	94228 (7)	111324 (20)	654 (5)
O(22′)	−31967 (14)	87924 (7)	124730 (18)	571 (4)
C(1′)	33595 (17)	84772 (7)	1745 (21)	421 (4)
C(2′)	39480 (20)	87729 (7)	−9031 (23)	458 (5)
C(3′)	46377 (19)	84276 (8)	−17780 (22)	458 (5)
C(4′)	52636 (20)	80043 (8)	−10740 (25)	485 (5)
C(5′)	46643 (20)	78064 (8)	1546 (23)	462 (5)
C(6′)	54799 (32)	75254 (12)	10585 (35)	681 (8)
C(7′)	44712 (28)	77145 (10)	−30463 (26)	589 (7)
C(8′)	36157 (42)	72873 (13)	−31050 (43)	803 (11)
C(9′)	51062 (52)	77995 (20)	−43262 (40)	844 (13)
O(3′)	38905 (15)	81529 (6)	−26337 (17)	545 (4)
O(4′)	53124 (19)	76181 (7)	−20486 (18)	628 (5)
O(5′)	42013 (13)	82124 (5)	9166 (15)	458 (3)

[a] $B_{iso} = {}^4/_3\sum_i\sum_j\beta_{ij}(a_i a_j)$. The esd's are given in parentheses.

I_{50} activity by an average of 8.9 times. Crystallographic and biological studies of the β-D-galactosides and β-D-glucosides synthesized previously[15] are in progress. Preliminary results show that the sugars of these glycosides also increase hog kidney Na^+,K^+-ATPase inhibitory activity by a nearly constant amount relative to the genin.

Conclusions

These structural results show that the A, B, and C rings of the steroid backbone have very little structural variation regardless of the nature of the C3 substituent. They also indicate that the D-ring conformation is quite flexible, and that the sugar substituent does not significantly alter the locations of the minimum-energy conformations of the C17β side group of the various analogues away from the "active" conformations of the corresponding genins.

Furthermore, the potential energy calculations for rotation about the bonds linking the steroid and sugar moieties reveal a relatively small amount of rotational freedom, especially for the α-D-rhamnoside sugar analogues. The structural results are consistent with these calculations, but show much less rotational freedom in the O3–C1′ bond than would be expected.

Combining these structural results with the hog kidney Na^+,K^+-ATPase inhibition data, we find that the same linear relationship between relative C17β-side-group carbonyl oxygen position and I_{50} observed for the genin analogues exists also for the glycosides. The addition of a sugar, however, enhances the relative activity by a constant factor depending on the nature of the sugar. The digitoxose acetonide derivatives have activity increased by a factor of 2, while the digitoxoside derivatives activity is increased by a factor of 8. While these results do not rule out an influence on activity by the O3′ oxygen's orientation, they are consistent with the earlier observation[6] that the orientation of the C4′ oxygen correlates well with activity.

Table VIII. Atomic Coordinates ($\times 10^5$) and Equivalent Isotropic Thermal Parameters ($\times 10^2$) for IIc[a]

	x	y	z	B_{iso}
C(1)	23807 (24)	61757 (7)	7890 (45)	433 (6)
C(2)	29111 (26)	61061 (6)	−10992 (57)	497 (8)
C(3)	28973 (24)	64337 (6)	−22745 (40)	393 (6)
C(4)	15570 (23)	66022 (6)	−22720 (32)	333 (5)
C(5)	9906 (21)	66667 (5)	−3565 (32)	301 (4)
C(6)	−3748 (23)	68287 (5)	−4936 (41)	375 (5)
C(7)	−13818 (21)	65705 (5)	−12206 (40)	356 (5)
C(8)	−14097 (19)	62294 (5)	−1035 (29)	262 (4)
C(9)	−363 (19)	60674 (5)	740 (28)	264 (4)
C(10)	9872 (21)	63314 (6)	8352 (29)	306 (4)
C(11)	−1107 (23)	57241 (6)	11758 (39)	361 (5)
C(12)	−10789 (23)	54705 (6)	3192 (36)	336 (5)
C(13)	−24811 (20)	56156 (5)	1663 (28)	275 (4)
C(14)	−24342 (19)	59697 (5)	−8714 (30)	267 (4)
C(15)	−22595 (28)	58596 (7)	−28655 (32)	371 (6)
C(16)	−31028 (37)	55315 (8)	−30951 (37)	502 (8)
C(17)	−32491 (23)	53658 (6)	−11465 (32)	321 (5)
C(18)	−31006 (28)	56421 (7)	20624 (34)	391 (6)
C(19)	6891 (36)	64292 (9)	28480 (37)	479 (7)
C(20)	−46455 (22)	53032 (6)	−6994 (36)	355 (5)
C(21)	−52071 (26)	49964 (7)	−4555 (39)	388 (6)
C(22)	−66559 (27)	49621 (7)	−2284 (43)	441 (6)
C(23)	−83803 (37)	45616 (13)	−1776 (76)	688 (12)
O(3)	38550 (16)	66720 (4)	−14797 (29)	399 (4)
O(14)	−37192 (15)	61175 (5)	−6563 (32)	421 (4)
O(22)	−73954 (23)	51964 (6)	−827 (63)	811 (10)
O(22′)	−69936 (20)	46241 (5)	−2480 (36)	543 (6)
C(1′)	43677 (21)	69064 (5)	−27209 (39)	357 (5)
C(2′)	49777 (29)	72096 (7)	−17072 (48)	450 (7)
C(3′)	56985 (25)	74509 (6)	−30202 (52)	465 (7)
C(4′)	65897 (25)	72465 (7)	−43055 (53)	492 (7)
C(5′)	58597 (29)	69420 (7)	−51751 (44)	457 (6)
C(6′)	67416 (51)	67174 (11)	−63730 (74)	721 (12)
O(3′)	47463 (22)	76418 (5)	−40401 (44)	568 (6)
O(4′)	70337 (23)	74869 (7)	−56631 (51)	724 (9)
O(5′)	53600 (16)	67251 (4)	−37432 (28)	405 (4)

[a] $B_{iso} = {}^4/_3\sum_i\sum_j\beta_{ij}(a_i a_j)$. The esd's are given in parentheses.

Experimental Section

Chemistry. The procedures for syntheses of all the genins, digitoxosides, and digitoxose acetonides have previously been reported.[1]

Biology. Hog kidney Na^+,K^+-ATPase (E.C. 3.6.1.3) was used to determine the inhibitory activity of the glycosides and genins as described in detail previously.[5,7] In brief, the inhibition was measured under type I equilibrium binding conditions (i.e., with Mg^{2+}, Na^+, ATP as the binding ligands with 10-min preincubation for genins and 2 h for glycosides. The resulting I_{50} (concentration required for 50% inhibition of the Na^+,K^+-ATPase) values are shown in Table IV. As described previously, all assays of Na^+,K^+-ATPase in the presence of genins or glycosides were carried out under equilibrium drug-binding conditions and in linear phases of the ATPase reaction.[5]

X-ray Crystal Structures. Intensity data for each structure determination were measured on a computer-controlled diffractometer using $\theta/2\theta$ scans. The structures were solved by using the direct methods program MULTAN[28] in conjunction with the NQEST figure of merit program.[29] Refinement of the coordinates of all atoms, anisotropic thermal parameters of the non-hydrogens and isotropic thermal parameters for the hydrogens using a full-matrix least-squares procedure was based on F with weights based on $1/\sigma^2_F$.

Crystal Data. (3β,5β,14β)-3-[(2′,6′-Dideoxy-3′,4′-*o*-(1′-methylethylidene)-β-D-*ribo*-hexopyranosyl)oxy]-14-hydroxycard-20(22)-enolide (Ib), $C_{32}H_{48}O_7$, has M_r = 544.7, orthorhombic space group $P2_12_12_1$, a = 16.025 (3) Å, b = 25.243 (7) Å, c = 7.637 (2) Å, Z = 4, d_c = 1.171 g cm^{-3}, μ(Mo Kα) = 0.874 cm^{-1}, R = 0.064 for 3074 observed data ($F > 4\sigma_F$). Data were measured to a $2\theta_{max}$ of 55° by using Mo Kα radiation (λ = 0.71069 Å) on a Syntex P_3 diffractometer yielding 4003 independent data. The final positional coordinates and equivalent isotropic

(28) Main, P.; Lessinger, L.; Woolfson, M. M.; Germain, G.; Declercq, J. P. "MULTAN 77. A System of Computer Programs for the Automatic Solution of Crystal Structures from X-ray Diffraction Data"; Universities of York, England, and Louvain, Belgium, 1977.

(29) DeTitta, G. T.; Edmonds, J. W.; Langs, D. A.; Hauptman, H. *Acta Crystallogr., Sect. A* **1975**, *A31*, 472–479.

Table IX. Atomic Coordinates ($\times 10^4$) and Equivalent Isotropic Thermal Parameters ($\times 10^2$) for IIIa[a]

	x	y	z	B_{iso}
C(1)	3428 (3)	2208 (2)	2695 (6)	320 (7)
C(2)	2534 (4)	1988 (2)	4179 (6)	363 (8)
C(3)	1186 (3)	1781 (2)	3017 (7)	357 (8)
C(4)	663 (3)	2440 (2)	1338 (7)	355 (8)
C(5)	1572 (3)	2641 (2)	−166 (6)	317 (7)
C(6)	965 (4)	3303 (2)	−1805 (6)	384 (8)
C(7)	863 (3)	4153 (2)	−760 (6)	346 (7)
C(8)	2175 (3)	4448 (2)	506 (5)	264 (6)
C(9)	2814 (3)	3779 (2)	2153 (5)	241 (6)
C(10)	2923 (3)	2912 (2)	1087 (5)	273 (6)
C(11)	4095 (3)	4102 (2)	3441 (6)	314 (7)
C(12)	3942 (3)	4960 (2)	4450 (6)	332 (7)
C(13)	3340 (3)	5640	2859 (5)	262 (6)
C(14)	2061 (2)	5309 (2)	1522 (5)	235 (5)
C(15)	1144 (3)	5363 (2)	3062 (5)	289 (6)
C(16)	1528 (3)	6174 (2)	4328 (5)	313 (7)
C(17)	2937 (3)	6386 (2)	4168 (5)	297 (6)
C(18)	4295 (3)	5882 (2)	1437 (6)	380 (8)
C(19)	3871 (3)	2958 (3)	−444 (6)	400 (8)
C(20)	3021 (3)	7252 (2)	3209 (6)	320 (7)
C(21)	2688 (3)	7975 (2)	4477 (6)	322 (7)
C(22)	2641 (3)	8830 (2)	3484 (6)	349 (7)
C(23)	3043 (4)	9601 (3)	558 (8)	481 (10)
C(24)	2416 (4)	7934 (3)	6410 (7)	465 (10)
O(3)	1118 (3)	986 (2)	1945 (5)	445 (7)
O(14)	1653 (2)	5908 (1)	−151 (4)	315 (5)
O(22)	2310 (3)	9463 (2)	4242 (5)	497 (7)
O(22′)	3011 (3)	8819 (2)	1635 (5)	428 (6)

[a] $B_{iso} = {}^4/_3\sum_i\sum_j\beta_{ij}(a_i a_j)$. The esd's are given in parentheses.

Table X. Atomic Coordinates ($\times 10^4$) and Equivalent Isotropic Thermal Parameters ($\times 10^2$) for IIIb[a]

	x	y	z	B_{iso}
C(1)	1669 (2)	4961 (4)	−1395 (4)	334 (7)
C(2)	1776 (2)	6209 (4)	−589 (5)	410 (9)
C(3)	1713 (2)	6160 (4)	1245 (5)	389 (8)
C(4)	952 (2)	5601 (4)	1498 (4)	319 (7)
C(5)	838 (2)	4341 (4)	715 (3)	258 (6)
C(6)	71 (2)	3799 (4)	1015 (3)	297 (6)
C(7)	−618 (2)	4442 (4)	32 (3)	280 (6)
C(8)	−568 (1)	4391 (3)	−1840 (3)	225 (5)
C(9)	196 (1)	4941 (4)	−2204 (3)	227 (5)
C(10)	912 (2)	4329 (3)	−1173 (3)	245 (5)
C(11)	222 (2)	4925 (5)	−4089 (3)	312 (7)
C(12)	−485 (2)	5499 (4)	−5075 (3)	286 (6)
C(13)	−1243 (2)	4918 (4)	−4784 (3)	257 (5)
C(14)	−1281 (1)	4939	−2894 (3)	225 (5)
C(15)	−1441 (2)	6267 (4)	−2569 (4)	298 (6)
C(16)	−1934 (2)	6733 (5)	−4151 (4)	400 (9)
C(17)	−1898 (2)	5796 (4)	−5527 (4)	297 (6)
C(18)	−1320 (2)	3651 (4)	−5520 (4)	381 (8)
C(19)	987 (2)	3014 (4)	−1733 (4)	332 (7)
C(20)	−2683 (2)	5209 (5)	−6143 (5)	431 (9)
C(21)	−3229 (2)	6094 (5)	−7046 (5)	458 (10)
C(22)	−3115 (2)	6371 (6)	−8804 (5)	499 (11)
C(23)	−3456 (6)	7689 (15)	−11081 (13)	1025 (37)
C(24)	−3797 (3)	6606 (9)	−6425 (7)	728 (21)
O(3)	2323 (2)	5413 (4)	2084 (4)	449 (6)
O(14)	−1943 (1)	4227 (4)	−2650 (3)	337 (5)
O(22)	−2718 (2)	5794 (6)	−9570 (5)	703 (12)
O(22′)	−3502 (2)	7347 (6)	−9379 (5)	731 (13)
C(1′)	2750 (2)	5932 (4)	3490 (4)	365 (7)
C(2′)	3145 (3)	4931 (5)	4568 (6)	467 (10)
C(3′)	3800 (2)	5369 (5)	5841 (5)	444 (9)
C(4′)	4254 (2)	6402 (6)	5310 (5)	464 (10)
C(5′)	3739 (2)	7335 (5)	4282 (5)	402 (9)
C(6′)	4175 (4)	8326 (7)	3614 (7)	597 (15)
C(7′)	4149 (2)	6561 (6)	8116 (5)	495 (11)
C(8′)	3827 (4)	7651 (7)	8873 (8)	669 (17)
C(9′)	4647 (4)	5763 (10)	9377 (9)	790 (22)
O(3′)	3525 (2)	5875 (4)	7259 (3)	461 (7)
O(4′)	4599 (2)	6903 (5)	6855 (4)	581 (9)
O(5′)	3297 (1)	6709 (4)	2916 (3)	406 (6)

[a] $B_{iso} = {}^4/_3\sum_i\sum_j\beta_{ij}(a_i a_j)$. The esd's are given in parentheses.

Table XI. Atomic Coordinates ($\times 10^4$) and Equivalent Isotropic Thermal Parameters ($\times 10^2$) for (20*S*)-IVb[a]

	x	y	z	B_{iso}
C(1)	−2935 (5)	7943 (2)	8548 (6)	333 (6)
C(2)	−1494 (5)	7975 (2)	7223 (5)	362 (6)
C(3)	263 (5)	8169 (2)	8642 (6)	351 (6)
C(4)	260 (4)	8999 (2)	10023 (6)	342 (6)
C(5)	−1186 (4)	8967 (2)	11371 (5)	294 (5)
C(6)	−1110 (5)	9806 (2)	12773 (5)	340 (6)
C(7)	−1587 (4)	10591 (2)	11415 (5)	316 (6)
C(8)	−3360	10436	9982	266 (5)
C(9)	−3523 (4)	9575 (2)	8605 (4)	265 (5)
C(10)	−3005 (4)	8772 (2)	9976 (5)	283 (5)
C(11)	−5341 (4)	9462 (2)	7256 (6)	338 (6)
C(12)	−5670 (5)	10238 (2)	5821 (5)	330 (6)
C(13)	−5553 (4)	11132 (2)	7050 (5)	277 (5)
C(14)	−3817 (4)	11246 (2)	8643 (5)	256 (5)
C(15)	−2523 (4)	11551 (2)	7221 (5)	307 (5)
C(16)	−3498 (5)	12222 (2)	5829 (6)	351 (6)
C(17)	−5395 (4)	11850 (2)	5343 (5)	291 (5)
C(18)	−7084 (5)	11184 (3)	8239 (6)	365 (6)
C(19)	−4328 (5)	8551 (3)	11446 (6)	380 (7)
C(20)	−6655 (4)	12572 (2)	5149 (5)	326 (6)
C(21)	−6235 (5)	13217 (2)	3454 (6)	403 (7)
C(22)	−8531 (5)	12266 (3)	4229 (8)	516 (10)
C(23)	−9153 (5)	12895 (2)	2582 (6)	426 (7)
O(3)	703 (4)	7483 (2)	10102 (4)	366 (5)
O(14)	−3994 (4)	11961 (2)	10120 (4)	323 (4)
O(21)	−7868 (4)	13440 (2)	2225 (5)	478 (6)
O(23)	−10620 (5)	12947 (2)	1638 (6)	608 (7)
C(1′)	1655 (4)	6837 (2)	9374 (5)	321 (6)
C(2′)	2527 (5)	6380 (3)	11313 (6)	398 (7)
C(3′)	3436 (5)	5602 (2)	10646 (6)	379 (6)
C(4′)	2466 (5)	5060 (2)	8706 (6)	377 (7)
C(5′)	1482 (5)	5616 (2)	6994 (6)	348 (6)
C(6′)	242 (5)	5066 (3)	5307 (7)	514 (9)
C(7′)	5404 (5)	5194 (2)	8577 (7)	423 (7)
C(8′)	6082 (6)	5583 (3)	6687 (8)	537 (10)
C(9′)	6682 (7)	4629 (4)	9894 (10)	639 (13)
O(3′)	4974 (4)	5893 (2)	9870 (5)	413 (5)
O(4′)	3830 (4)	4668 (2)	7865 (5)	448 (6)
O(5′)	514 (4)	6223 (2)	7990 (5)	357 (4)

[a] $B_{iso} = {}^4/_3\sum_i\sum_j\beta_{ij}(a_i a_j)$. The esd's are given in parentheses.

thermal parameters for the non-hydrogen atoms are given in Table V.

(3β,5β,14β,20*E*)-Methyl 14-hydroxylpregn-20-ene-21-carboxylate (IIa) monohydrate, $C_{23}H_{36}O_4 \cdot H_2O$, has M_r = 394.6, orthorhombic space group $P2_12_12_1$, a = 16.5559 (2) Å, b = 17.999 (1) Å, c = 7.2666 (4) Å, Z = 4, d_c = 1.210 g cm^{-3}, μ(Cu Kα) = 6.764 cm^{-1}, R = 0.051 for 1675 observed data ($I > 2\sigma_I$). Data were measured to a $2\theta_{max}$ of 116° using Cu Kα radiation (λ = 1.5418 Å) on a Syntex P_3 diffractometer yielding 1709 independent data. The final positional coordinates and equivalent isotropic thermal parameters for the non-hydrogen atoms are given in Table VI.

(3β,5β,14β,20*E*)-Methyl 3-[(2′,6′-dideoxy-3′,4′-*o*-(1′-methylethylidene)-β-D-*ribo*-hexopyranosyl)oxy]-14-hydroxylpregn-20-ene-21-carboxylate (IIb), $C_{32}H_{50}O_7$, has M_r = 546.8, orthorhombic space group $P2_12_12_1$, a = 11.758 (4) Å, b = 26.573 (3) Å, c = 10.131 (4) Å, Z = 4, d_c = 1.147 g cm^{-3}, μ(Cu Kα) = 6.452 cm^{-1}, R = 0.039 for 3418 observed data ($F > 3\sigma_F$). Data were measured to a $2\theta_{max}$ of 150° using Cu Kα radiation (λ = 1.5418 Å) on an Enraf-Nonius CAD-4 diffractometer yielding 3667 independent data. The final positional coordinates and equivalent isotropic thermal parameters for the non-hydrogen atoms are given in Table VII.

(3β,5β,14β,20*E*)-Methyl 3-[(2′,6′-dideoxy-β-D-*ribo*-hexopyranosyl)-oxy]-14-hydroxylpregn-20-ene-21-carboxylate (IIc), $C_{29}H_{46}O_7$, has M_r = 506.7, orthorhombic space group $P2_12_12_1$, a = 10.2354 (5) Å, b = 38.154 (2) Å, c = 7.3000 (3) Å, Z = 4, d_c = 1.180 g cm^{-3}, μ(Cu Kα) = 6.774 cm^{-1}, R = 0.044 for 3122 observed data ($F > 4\sigma_F$). Data were measured to a $2\theta_{max}$ of 150° using Cu Kα radiation (λ = 1.5418 Å) on an Enraf-Nonius CAD-4 diffractometer yielding 3364 independent data. The final positional coordinates and equivalent isotropic thermal parameters for the non-hydrogen atoms are given in Table VIII.

(3β,5β,14β,20*E*)-Methyl 14-hydroxyl-21-methylenepregn-21-carboxylate (IIIa), $C_{24}H_{38}O_4$, has M_r = 390.6, monoclinic space group $P2_1$, a = 10.628 (2) Å, b = 15.951 (2) Å, c = 6.418 (1) Å, β = 102.12 (3)°, Z = 2, d_c = 1.219 g cm^{-3}, μ(Mo Kα) = 0.872 cm^{-1}, R = 0.072 for 2523 observed data ($F > 2\sigma_F$). Data were measured to a $2\theta_{max}$ of 60° using Mo Kα radiation (λ = 0.71069 Å) on a Syntex P_3 diffractometer

yielding 3210 independent data. The final positional coordinates and equivalent isotropic thermal parameters for the non-hydrogen atoms are given in Table IX.

(3β,5β,14β,20*E*)-Methyl 3-[(2′,6′-dideoxy-3′,4′-*o*-(1′-methylethylidene)-β-D-*ribo*-hexopyranosyl)oxy]-14-hydroxyl-21-methylenepregn-21-carboxylate (IIIb), $C_{33}H_{52}O_7$, has M_r = 560.8, monoclinic space group $P2_1$, a = 17.621 (3) Å, b = 11.077 (3) Å, c = 8.115 (2) Å, β = 98.60 (2)°, Z = 2, d_c = 1.189 g cm^{-3}, μ(Mo Kα) = 0.881 cm^{-1}, R = 0.058 for 4073 observed data ($F > 4\sigma_F$). Data were measured to a $2\theta_{max}$ of 60° using Mo Kα radiation (λ = 0.71069 Å) on a Syntex P_3 diffractometer yielding 4826 independent data. The final positional coordinates and equivalent isotropic thermal parameters for the non-hydrogen atoms are given in Table X.

3-[(2′,6′-Dideoxy-3′,4′-*o*-(1′-methylethylidene)-β-D-*ribo*-hexopyranosyl)oxy](20*S*)-20,22-dihydrodigitoxigenin ((20*S*)-IVb), $C_{32}H_{50}O_7$, has M_r = 546.8, triclinic space group P_1, a = 7.887 (1) Å, b = 15.350 (2) Å, c = 6.303 (1) Å, α = 91.80 (1), β = 99.84 (1), γ = 93.53 (1)°, Z = 1, d_c = 1.211 g cm^{-3}, μ(Cu Kα) = 6.811 cm^{-1}, R = 0.046 for 3000 observed data ($F > 3\sigma_F$). Data were measured to a $2\theta_{max}$ of 150° using Cu Kα radiation (λ = 1.5418 Å) on an Enraf-Nonius CAD-4 diffractometer yielding 3058 independent data. The final positional coordinates and equivalent isotropic thermal parameters for the non-hydrogen atoms are given in Table XI.

Conformational Energy Calculations. Potential energy calculations for rotations of the C3-O3 and O3-C1′ steroid-sugar linkage bonds were done using the molecular mechanics program CAMSEQ[30] in conjunction with the modeling and graphics features of the NIH PROPHET computer system.[31] The potential energies were calculated at 10° rotation steps of each bond, while holding the geometry fixed as observed in the crystal structure. The final energies were then adjusted so the minimum value was zero.

Acknowledgment. This research was supported in part by research Grant HL-21457 awarded by the National Heart, Lung and Blood Institute, DHHS, and by the Medical Research Fund of the Veterans Administration. Analysis of data was expedited using the PROPHET system, a national computer resource supported by the NIH.

Supplementary Material Available: Tables of atomic coordinates and anisotropic thermal parameters and hydrogen atom coordinates and isotropic thermal parameters for Ib, IIa-c, IIIa,b, and (20*S*)-IVb (14 pages). Ordering information is given on any current masthead page.

(30) Weintraub, H. J. R.; Hopfinger, A. J. *Int. J. Quantum Chem., Quantum Biol. Symp.* **1975**, *2*, 203-208.
(31) Weeks, C. M.; Cody, V.; Pokrywiecki, S.; Rohrer, D. C.; Duax, W. L. *AFIPS Natl. Comput. Conf. Expo. Conf. Proc.* **1974**, *43*, 469-472.

Origin of Benzophenone Ketyl in Reactions of Benzophenone with Lithium Dialkylamides. Implications for Other Possible Electron-Transfer Reactions†

Martin Newcomb*[1] and Michael T. Burchill

Contribution from the Department of Chemistry, Texas A&M University, College Station, Texas 77843. *Received May 31, 1984*

Abstract: A reaction scheme is presented for the formation of benzophenone ketyl in reactions of lithium dialkylamides containing β-hydrogen atoms with benzophenone. The key steps are fast concerted β-hydride reduction of benzophenone to give lithium benzhydrolate, rate-limiting deprotonation of the lithium benzhydrolate to give dilithium benzophenone dianion, and fast electron transfer from the dianion to benzophenone to give two molecules of ketyl. Benzophenone is supplied throughout the course of the reaction by a retro-aldol reaction of the lithium salt of aldol-like adduct **4** formed early in the reaction. The reaction scheme was confirmed by kinetic studies of the individual steps. The velocity of the retro-aldol reaction was orders of magnitude faster than that of ketyl formation. The deprotonation of lithium benzhydrolate by lithium diisopropylamide (LDA) in tetrahydrofuran at 22 °C occurred with an apparent second-order rate constant which was approximately equal to one-half of the apparent second-order rate constant for ketyl formation when benzophenone was treated with LDA under similar conditions. The possibility that related sequences of reactions could occur when weak organic oxidants are treated with reagents that can act as hydride donors and bases is discussed.

The reduction of benzophenone by lithium dialkylamides was first reported two decades ago by Wittig who concluded that the mechanism of the reaction involved a concerted β-hydride transfer from the base to benzophenone.[2] More recent studies, however, provided evidence that the reaction of amide bases with ketones may involve an electron-transfer step (single electron transfer, SET) from base to ketone. For example, Scott et al.[3a] observed that benzophenone ketyl coupling products were formed in the reaction of lithium diisopropylamide (LDA) with benzophenone. Although Scott made no mechanistic claims, it was clear that some route to the odd-electron radical anion existed. Ashby et al.[3b] studied the reactions of benzophenone and dimesityl ketone with LDA and concluded that the detection of ketyl by ESR (in up to 35% yield in the case of benzophenone) during the course of the reactions was evidence for an SET pathway. A pinacol product has also been reported by Paquette et al. from the reaction of LDA with an aliphatic diketone,[4] and an SET mechanism for the reaction of LDA with an ynone has been suggested.[5] Primarily because of the large percentage of ketyl detected in the reaction of LDA with benzophenone, this reaction had begun to assume the role of an archetypal SET process.

† Dedicated to Professor D. J. Cram on the occasion of his 65th birthday in admiration of his fundamental contributions in mechanistic carbanion chemistry.

(1) Camille and Henry Dreyfus Teacher-Scholar, 1980-1985.
(2) (a) Wittig, G.; Schmidt, H.-J.; Renner, H. *Chem. Ber.* **1962**, *95*, 2377-2383. (b) Wittig, G.; Frommeld, H.-D. *Chem. Ber.* **1964**, *97*, 3541-3548. (c) Wittig, G.; Reiff, H. *Angew. Chem., Int. Ed. Eng.* **1968**, *7*, 7-14. (d) Wittig, G.; Ebel, H. F.; Häusler, G. *Justus Liebigs Ann. Chem.* **1971**, *743*, 120-143.
(3) (a) Scott, L. T.; Carlin, K. J.; Schultz, T. H. *Tetrahedron Lett.* **1978**, 4637-4638. (b) Ashby, E. C.; Goel, A. B.; DePriest, R. N. *Tetrahedron Lett.* **1981**, *22*, 4355-4358.
(4) Balogh, D. W.; Paquette, L. A.; Engel, P.; Blount, J. F. *J. Am. Chem. Soc.* **1981**, *103*, 226-228. Paquette, L. A.; Balogh, D. W. *J. Am. Chem. Soc.* **1982**, *104*, 774-783.
(5) Shen, C. C.; Ainsworth, C. *Tetrahedron Lett.* **1979**, 89-92.

0002-7863/84/1506-8276$01.50/0